

General Disclaimer

One or more of the Following Statements may affect this Document

- This document has been reproduced from the best copy furnished by the organizational source. It is being released in the interest of making available as much information as possible.
- This document may contain data, which exceeds the sheet parameters. It was furnished in this condition by the organizational source and is the best copy available.
- This document may contain tone-on-tone or color graphs, charts and/or pictures, which have been reproduced in black and white.
- This document is paginated as submitted by the original source.
- Portions of this document are not fully legible due to the historical nature of some of the material. However, it is the best reproduction available from the original submission.

**ADVANCED METHODS FOR
PREPARATION AND CHARACTERIZATION
OF INFRARED DETECTOR MATERIALS**

J. G. Broerman

B. J. Morris

P. J. Meschter

**McDonnell Douglas Research Laboratories
St. Louis, Missouri 63166**

15 February 1983

**Final Report for the period 30 September 1981 - 15 February 1983
Contract NAS8-33107**

**Prepared for
George C. Marshall Space Flight Center
Marshall Space Flight Center, Alabama 35812**

MCDONNELL DOUGLAS RESEARCH LABORATORIES

MCDONNELL DOUGLAS



(NASA-CR-170798) ADVANCED METHODS FOR
PREPARATION AND CHARACTERIZATION OF INFRARED
DETECTOR MATERIALS Final Report, 30 Sep.
1981 - 15 Feb. 1983 (McDonnell-Douglas
Research Labs.) 28 p HC A03/MF A01 CSCI 20L G3/76

N83-30271

**Unclas
28212**



PREFACE

This report presents the results of research performed from 30 September 1981 through 15 February 1983 by the McDonnell Douglas Research Laboratories (MDRL) under the National Aeronautics and Space Administration Contract NAS8-33107 entitled "Advanced Methods for the Preparation and Characterization of Infrared Detector Materials." The ultimate objectives of the study are to quantitatively establish the characteristics of $\text{Hg}_{1-x}\text{Cd}_x\text{Te}$ as grown on Earth as a basis for subsequent evaluation of the material processed in space and to develop the experimental and theoretical analytical methods required for such evaluation.

The work was performed in the Solid State Sciences Department, managed by Dr. C. R. Whitsett. The principal investigator from 30 September 1981 until 31 March 1982 was Dr. S. L. Lehoczky, who resigned from MDRL on 31 March 1982 to accept employment by the NASA George C. Marshall Space Flight Center. Dr. J. G. Broerman replaced Dr. S. L. Lehoczky as principal investigator on 1 April 1982. The co-investigators were Dr. B. J. Morris and Dr. P. J. Meschter. The technical manager was Mr. Val Fogle, NASA, George C. Marshall Space Flight Center.

During the time that he was principal investigator, Dr. S. L. Lehoczky charged 508 h to the contract for work primarily on the theory of the phase equilibria for the ternary Hg-Cd-Te alloy system, and the results of his investigation are not included in this report.

This report has been reviewed and is approved.

C. R. Whitsett by D. P. Ames
C. R. Whitsett
Chief Scientist-Solid State Sciences
McDonnell Douglas Research Laboratories

D. P. Ames
D. P. Ames
Staff Vice President
McDonnell Douglas Research Laboratories

Val Fogle
Val Fogle
Technical Manager
NASA George C. Marshall
Space Flight Center

CONTENTS

	<u>Page</u>
1. INTRODUCTION.....	1
1.1 Scope of Study.....	1
1.2 Summary of Progress.....	1
1.2.1 Previously Reported Progress for the Period 5 December 1978-5 July 1980.....	1
1.2.2 Previously Reported Progress for the Period 5 July 1980-30 September 1981.....	3
1.2.3 Progress for the Current Period 30 September 1981-15 February 1983.....	4
1.3 Formal Reports, Publications, and Presentations.....	4
1.3.1 Research Funded Under Contract NAS8-33107.....	4
1.3.2 Research Funded in Part Under Contract NAS8-33107.....	5
2. TERNARY Hg-Cd-Te PHASE DIAGRAM.....	6
2.1 Alloy Preparation.....	6
2.2 Experimental Method for Differential Thermal Analysis.....	7
2.3 Differential Thermal Analysis Results for the Hg-Rich Region of the Ternary System.....	9
3. DIRECTIONAL SOLIDIFICATION OF $\text{Hg}_{1-x}\text{Cd}_x\text{Te}$ ALLOYS FROM PSEUDOBINARY MELTS.....	12
3.1 Alloy Preparation.....	12
3.2 Procedure for Directional Solidification.....	12
3.3 Determination of Alloy Composition by Mass Density Measurements.....	16
3.4 Determination of Alloy Composition by Infrared Transmission Measurements.....	18
3.5 Electrical Characterization.....	19
REFERENCES.....	23

PRECEDING PAGE BLANK NOT FILMED

LIST OF ILLUSTRATIONS

<u>Figure</u>	<u>Page</u>
1. $(\text{Hg}_{1-x}\text{Cd}_x)_y\text{Te}_{1-y}$ samples prepared.....	7
2. Experimental arrangement for differential thermal analysis measurements.....	8
3. Electronic instrumentation and furnace control for differential thermal analysis.....	8
4. Thermogram of typical HgCdTe differential thermal analysis experiment.....	10
5. Bridgman-Stockbarger crystal-growth furnace assembly.....	13
6. Furnace temperature profile for sample L0750-27.....	14
7. Furnace temperature profile for sample L0750-35.....	15
8. Furnace temperature profile for sample L0750-38.....	15
9. Composition profile of sample L0750-27.....	17
10. Composition profile of sample L0750-38.....	18
11. Radial composition of sample L0721-37-1.....	20
12. Radial composition of sample L0721-37-2.....	20
13. Block diagram of automated system for measurement of galvanomagnetic properties of semiconductors.....	21
14. Hall electron concentration for sample L0721-37-2.....	22
15. Hall electron mobility for sample L0721-37-2.....	22

LIST OF TABLES

<u>Table</u>	<u>Page</u>
1. Liquidus temperatures for Hg-rich $(\text{Hg}_{1-x}\text{Cd}_x)_y\text{Te}_{1-y}$ alloys.....	11
2. Crystal growth parameters.....	16
3. Crystal growth parameters for ingot L0721-37.....	19

1. INTRODUCTION

1.1 Scope of Study

The overall study includes the entire range, $0 < x < 1$, of $\text{Hg}_{1-x}\text{Cd}_x\text{Te}$ alloy compositions. Crystals were prepared by the Bridgman-Stockbarger method with a wide range of crystal growth rates and temperature gradients adequate to prevent constitutional supercooling under diffusion-limited, steady-state, growth conditions. The longitudinal compositional gradients for different growth conditions and alloy compositions were calculated and compared with experimental data to develop a quantitative model of solute redistribution during the crystal growth of the alloys. Measurements were performed to ascertain the effect of growth conditions on radial compositional gradients. The pseudobinary HgTe-CdTe constitutional phase diagram was determined by precision differential-thermal-analysis measurements and used to calculate the segregation coefficient of Cd as a function of x and interface temperature. Experiments were conducted to determine the ternary phase equilibria in selected regions of the Hg-Cd-Te constitutional phase diagram. Electron and hole mobilities as functions of temperature were analyzed to establish charge-carrier scattering probabilities. Computer algorithms specific to $\text{Hg}_{1-x}\text{Cd}_x\text{Te}$ were developed for calculations of the charge-carrier concentrations, charge-carrier mobilities, Hall coefficient, and Fermi energy as functions of x , temperature, ionized donor and acceptor concentrations, and neutral defect concentrations.

1.2 Summary of Progress

1.2.1 Previously Reported Progress for the Period 5 December 1978 - 5 July 1980 (Reference 1)

A series of differential-thermal-analysis (DTA) measurements was performed for $\text{Hg}_{1-x}\text{Cd}_x\text{Te}$ alloy compositions with $x = 0, 0.1, 0.2, 0.3, 0.4, 0.6, 0.7, 0.8, 0.9$, and 1.0 . The liquidus and solidus temperatures deduced from the DTA data were used to establish the pseudobinary HgTe-CdTe constitutional phase diagram.¹⁻³ The segregation coefficient of Cd was determined as a function of x and interface temperature.

ORIGINAL PAGE IS
OF POOR QUALITY

Iterative phase-equilibrium calculations based on the regular associated solution (RAS) theory⁴⁻⁵ were performed, and a set of RAS parameters was obtained by simultaneously least-squares-fitting the binary Hg-Te⁶ and Cd-Te⁷⁻⁹ and pseudobinary HgTe-CdTe phase diagrams.¹⁰ The RAS parameters were used to calculate the activities of Hg, Cd, and Te₂ and their partial pressures over pseudobinary melts.

Hg_{1-x}Cd_xTe alloy crystals were grown by the Bridgman-Stockbarger method with constant furnace-translation rates of 0.0685 to 5.62 $\mu\text{m/s}$. For three Hg_{0.8}Cd_{0.2}Te ingots, the longitudinal compositional profiles were determined by precision density measurements and were compared with calculated profiles¹¹ for various assumed values of D, the liquid HgTe-CdTe interdiffusion coefficient. The best fits to the data for the alloys with $x = 0.2$ yielded $5.5 \times 10^{-5} \text{ cm}^2/\text{s}$ for D and $1.5 \times 10^6 \text{ K}\cdot\text{s}/\text{cm}^2$ for G/R, the interface-temperature-gradient to growth-rate ratio required to prevent constitutional supercooling in the melt during crystal growth of Hg_{0.8}Cd_{0.2}Te alloys.^{1,3,12} Radial compositional variations were measured on thin slices from a series of ingots by infrared (IR) transmission-edge mapping. The radial compositional profiles deduced from the cut-on wavelengths implied concave solid/liquid interfaces for the entire lengths of the crystals.

Theoretical models and computer programs specific to Hg_{1-x}Cd_xTe were developed for calculations of charge-carrier concentrations, Hall coefficient, Fermi energy, and conduction-electron mobility as functions of x, temperature, and ionized-defect and neutral-defect concentrations. As in previous work on the HgCdSe alloy system,^{13,14} the Kane three-band model¹⁵ was used to describe the band structure of the HgCdTe alloys, and the best available band parameters were compiled from the literature. The temperature dependence of the electron concentration was calculated for various net donor concentrations from 4.2 to 300 K, and the calculated results agree well with available experimental data.¹

The mobility calculations included the following intrinsic scattering mechanisms: longitudinal-optical phonon, longitudinal- and transverse-acoustical phonon, heavy-hole, and alloy disorder potential. The extrinsic scattering mechanisms included charge and neutral point-defects. A comparison of calculated results with available experimental data indicates that

ORIGINAL PAGE IS
OF POOR QUALITY

longitudinal-optical phonon scattering and charged and neutral defect scattering are the dominant mobility-limiting mechanisms.

1.2.2 Previously Reported Progress for the Period 5 July 1980-
30 September 1981 (Reference 16)

A series of differential-thermal-analysis measurements was performed for $(\text{Hg}_{1-x}\text{Cd}_x)_y\text{Te}_{1-y}$ alloy compositions with $x = 0.091$ and $y = 0.648$; $x = 0.100$ and $y = 0.550$ and 0.591 ; $x = 0.200$ and $y = 0.544, 0.554, 0.60,$ and 0.952 ; $x = 0.299$ and $y = 0.544$ and 0.589 ; and $x = 0.401$ and $y = 0.545$. The DTA data were used to establish the liquidus temperatures for the alloy compositions.

The pseudobinary data obtained during the previous funding period were refitted to a set of empirical equations to obtain more accurate expressions for the segregation coefficient of Cd as a function of x and interface temperature than was given in Reference 1. Preliminary theoretical analysis was performed to establish the ternary phase equilibrium parameters for the metal-rich region of the phase diagram. Pseudobinary HgTe-CdTe phase equilibrium calculations were performed to determine the sensitivity of the thermodynamic fitting parameters to various assumptions used in the calculational models.^{1,4,5}

$\text{Hg}_{0.8}\text{Cd}_{0.2}\text{Te}$ alloy crystals were grown by a Bridgman-Stockbarger method at constant furnace-translation rates of $0.241, 0.245,$ and $0.247 \mu\text{m/s}$, and a $\text{Hg}_{0.7}\text{Cd}_{0.3}\text{Te}$ alloy crystal was grown at a furnace translation rate of $0.231 \mu\text{m/s}$. The lower-zone temperatures ranged from 175 to 600°C , and the upper-zone temperatures ranged from 810 to 920°C . Radial compositional variations were measured on thin slices from the ingots by infrared transmission mapping. Similar measurements were performed for an ingot grown during the previous contractual period. The radial alloy homogeneities of the ingots showed a strong correlation to the growth parameters employed. The variation of the radial compositional distributions with changes in the upper- and lower-zone temperatures suggests significantly higher thermal conductivities in the melt than in the solidified alloys.

Galvanomagnetic measurements were performed to expand the data base for well-characterized, homogeneous HgCdTe crystals. Using the van der Pauw technique, Hall coefficient and resistivity measurements from 10 to 300 K were performed on slices from 10-mm and 5-mm diameter ingots. For a number of

ORIGINAL PAGE IS
OF POOR QUALITY

slices the measurements were repeated following annealing in a mercury atmosphere at several temperatures. Theoretical analyses were performed to estimate point-defect concentrations in n-type samples.

1.2.3 Progress for the Current Period: 30 September 1980-15 February 1983

A series of differential-thermal-analysis measurements was performed for $(\text{Hg}_{1-x}\text{Cd}_x)_y\text{Te}_{1-y}$ alloy compositions with $x = 0.2$, $y = 0.5, 0.7$, and 0.8 ; $x = 0.1$, $y = 0.75$ and 0.85 ; $x = 0.3$, $y = 0.7, 0.8$, and 0.9 ; $x = 0.4$, $y = 0.75$ and 0.85 . The DTA data were used to determine liquidus temperatures for the alloy compositions. A slightly different method of sample equilibrating and data recording was employed that yields sharper thermograms.

$\text{Hg}_{1-x}\text{Cd}_x\text{Te}$ alloy crystals were grown by the Bridgman-Stockbarger method. The sample compositions grown were $x = 0.2, 0.5$, and 0.7 at constant furnace translation rates of $0.59, 1.2$, and $0.35 \mu\text{m/s}$, respectively. The lower-zone temperature ranged from $500\text{--}650^\circ\text{C}$, and the upper-zone temperature ranged from 815 to 1070°C . Longitudinal compositional profiles were obtained from the $x = 0.2$ and 0.7 samples by mass density measurements. The samples as grown were highly p-type, and attempts to convert the samples to n-type by annealing so that they were sufficiently transparent for IR radial compositional mapping failed. Another low-growth-rate ($0.23 \mu\text{m/s}$) sample with $x = 0.3$ grown under the MDC IRAD program was annealed and IR composition profiled.

1.3 Formal Reports, Publications, and Presentations:

1.3.1 Research Funded Under Contract NAS8-33107:

- F. R. Szofran and S. L. Lehoczky, "The HgTe-CdTe Pseudobinary Phase Diagram", 22nd Annual Electronic Materials Conference, Ithaca, New York, 24-27 June 1980.
- S. L. Lehoczky, F. R. Szofran, and B. G. Martin, "Advanced Methods for Preparation and Characterization of Infrared Detector Materials", McDonnell Douglas Corporation Report MDC Q0717 (5 July 1980), Final Report for the period 5 December 1978 - 5 July 1980 for the George C. Marshall Space Flight Center Contract No. NAS8-33107.

ORIGINAL PAGE IS
OF POOR QUALITY

- S. L. Lehoczky and F. R. Szofran, "Directional Solidification and Characterization of $\text{Hg}_{1-x}\text{Cd}_x\text{Te}$ Alloys", Materials Research Society Symposium - Materials Processing Research in the Reduced Gravity Environment of Space, Boston, Massachusetts, 16-18 November 1981.
- S. L. Lehoczky and F. R. Szofran, "Diffusion-Limited Directional Solidification of $\text{Hg}_{0.8}\text{Cd}_{0.2}\text{Te}$ ", Fifth International Conference on Vapor Growth and Epitaxy and Fifth American Conference on Crystal Growth, Coronado, California, 19-24 July 1981.
- S. L. Lehoczky and F. R. Szofran, "Advanced Methods for Preparation and Characterization of Infrared Detector Materials", McDonnell Douglas Corporation Report MDC Q0744 (30 September 1981), Final Report for the period 5 July 1980-30 September 1981 for the George C. Marshall Space Flight Center Contract No. NAS8-33107.

1.3.2 Research Funded in Part Under Contract NAS8-33107

- F. R. Szofran and S. L. Lehoczky, "The Pseudobinary HgTe-CdTe Phase Diagram", J. Electron. Matl. 10, 1131 (1981).
- S. L. Lehoczky, C. J. Summers, and F. R. Szofran, "Directional Solidification and Characterization of $\text{Hg}_{1-x}\text{Cd}_x\text{Te}$ ($x < 0.25$)", NATO Cadmium Mercury Telluride (CMT) Workshop, Grenoble, France, 23-24 April 1981.
- S. L. Lehoczky, F. R. Szofran, C. J. Summers, and B. G. Martin, "Electrical Characterization of $\text{Hg}_{1-x}\text{Cd}_x\text{Te}$ Alloys", Materials Research Society Symposium - Materials Processing Research in the Reduced Gravity Environment of Space, Boston, Massachusetts, 16-18 November 1981.

2. TERNARY Hg-Cd-Te PHASE DIAGRAM

Differential-thermal-analysis (DTA) measurements on ternary $(\text{Hg}_{1-x}\text{Cd}_x)_y\text{Te}_{1-y}$ alloys were continued with the objective of establishing accurate liquidus temperatures in the mercury-rich composition region $0.1 \leq x \leq 0.4$, $0.7 \leq y \leq 0.9$.

2.1 Alloy Preparation

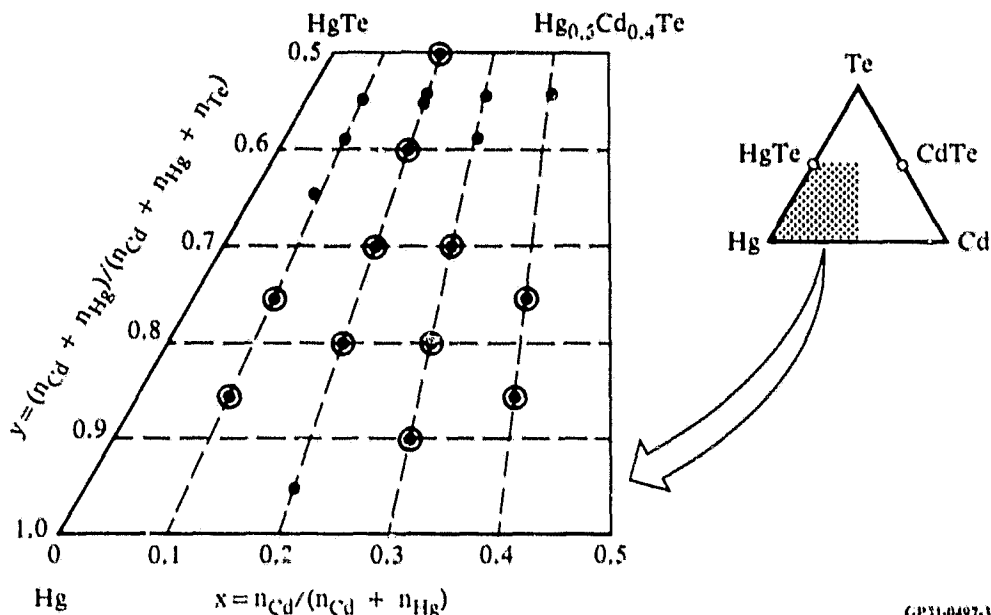
The Hg-Cd-Te ternary alloys used for the DTA measurements were prepared by reacting the constituent elements in sealed fused silica ampules, 5 mm i.d. by 10 mm o.d. The ampules were etched in aqueous HF and annealed in vacuum at 1150°C to remove residual contaminants before filling. Cd bars were cut from large ingots (99.9999% pure), etched in HNO_3 , and repeatedly rinsed in methanol.

The Te was prepared by crushing large ingots (99.9999% pure) in an agate mortar in a dry nitrogen atmosphere. The ampules were then loaded in a vertical position first with 99.99999% pure Hg, then Te powder, and finally with the Cd bar to prevent contact between Hg and Cd in air.

The loaded ampules were backfilled with He and evacuated several times before being sealed in vacuum. After sealing, the ampules were flame annealed until no sign of stress fringes was observed under polarized light. This procedure, along with the selection of high-quality, striation-free quartz, was found to be necessary to avoid explosions during liquid-phase equilibration of the sample or during the subsequent DTA run.

After loading and sealing, the ampules were placed in a sealed Inconel cylinder in a tube furnace, heated at $2^\circ\text{C}/\text{min}$ to a temperature $15\text{--}50^\circ\text{C}$ above the estimated liquidus temperature, and held at that temperature for 16 h to ensure sample homogenization. The samples were then removed from the furnace and allowed to cool on the bench to room temperature. This procedure protected the DTA apparatus by allowing most explosions caused by imperfections in the ampule to occur during homogenization. The ternary compositions prepared during this contract period are shown in Figure 1 along with the compositions already reported in Reference 16.

- ⊙ Liquidus temperature determined this report
- Liquidus temperature previously determined (Ref. 16)



GP31-0497.3

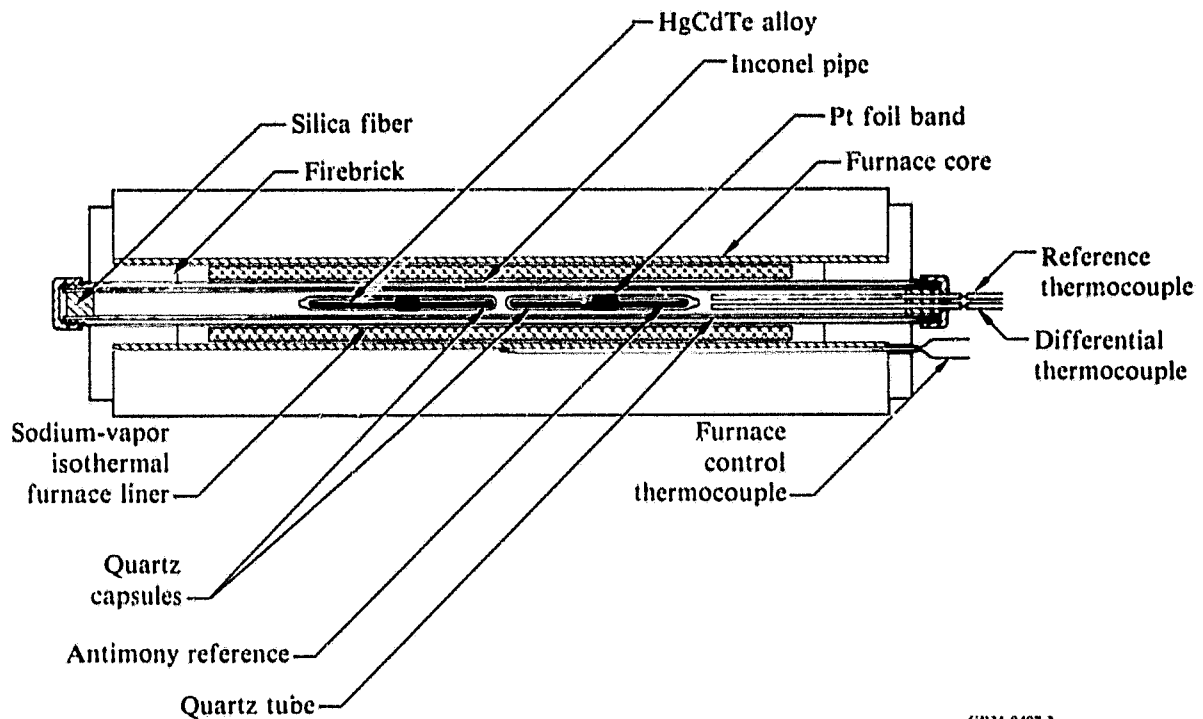
Figure 1. $(\text{Hg}_{1-x}\text{Cd}_x)_y\text{Te}_{1-y}$ samples prepared.

2.2 Experimental Method for Differential Thermal Analysis

The experimental apparatus for the DTA measurements is shown in Figure 2. The ampule containing the alloy sample and an ampule containing antimony were mounted in a 25 mm o.d. quartz tube serving as a centering fixture. The quartz tube was mounted coaxially in an inconel tube which protected the rest of the system in the event of explosion, and this assembly was mounted in a 610-mm long tube furnace lined with a 460-mm long heat pipe.

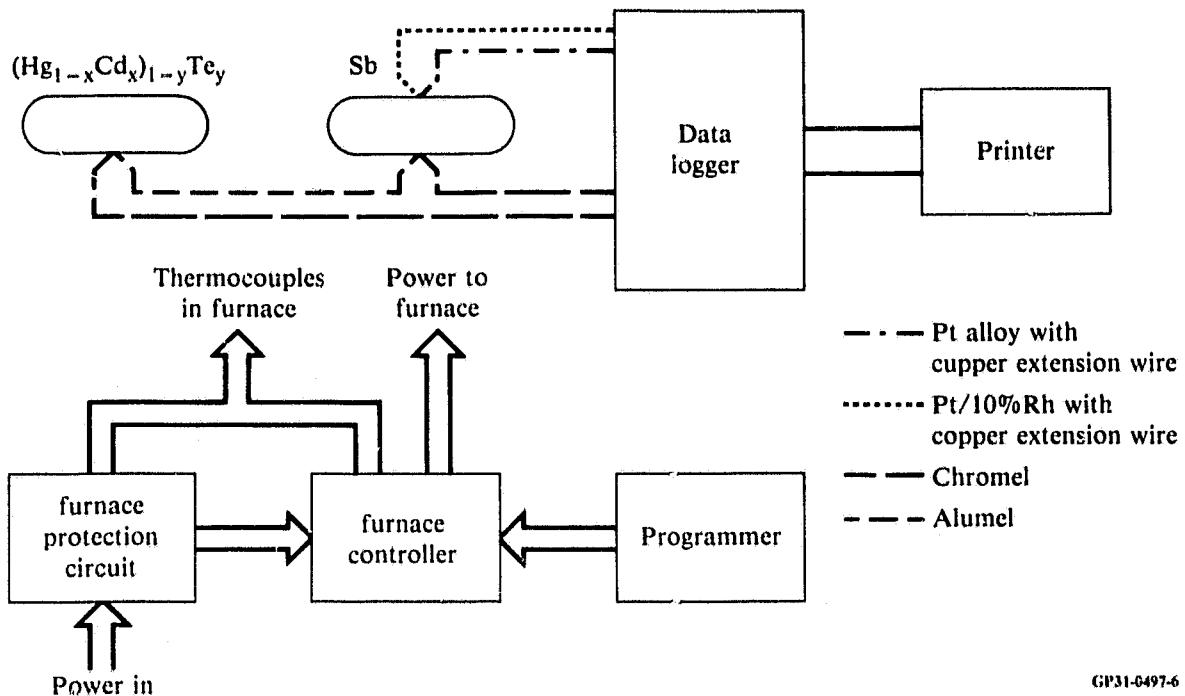
The alloy and reference Sb ampules were fitted with 5-mm wide Pt-foil bands located near the middle of the ampules. The two junctions of a type-K (chromel-alumel) differential thermocouple were secured to the bands and a second type-S (Pt/Pt-10Rh) thermocouple was secured to the band on the reference Sb ampule. The output of both thermocouples was connected to a data logger (Fluke 2240B) with isothermal, thermally-compensated junctions. The absolute temperature and differential thermocouple emf were printed out each minute by the data logger. The differential thermocouple was replaced for each DTA sample. A diagram of the electronic instrumentation is shown in Figure 3.

ORIGINAL PAGE IS
OF POOR QUALITY



GP31-0497-2

Figure 2. Experimental arrangement for differential thermal analysis measurements.



GP31-0497-6

Figure 3. Electronic instrumentation and furnace control for differential thermal analysis.

To begin a DTA run, the sample assembly was heated at $2^{\circ}\text{C}/\text{min}$ to a temperature 50°C below the anticipated liquidus temperature. During heating, the melting temperature of the Sb-reference ampule was observed. This temperature was always within 0.8°C of the best evaluated Sb melting temperature¹⁷ of 630.8°C (Reference 3). The HgCdTe ampule was held above the solidus temperature and 50°C below the anticipated liquidus temperature for at least 16 h to ensure equilibration. The assembly was then heated at $2^{\circ}\text{C}/\text{min}$ until a break in the differential temperature curve denoted the liquidus. These breaks were steeper than seen in our previous experiments^{1,16} and a typical example is shown in Figure 4. The sample was then cooled to the solid and liquid range, held for 16 h and the process repeated. Liquidus temperatures on successive runs on the same ampule agreed to within 2°C .

2.3 Differential Thermal Analysis Results for The Hg-Rich Region of the Ternary System

Liquidus temperatures obtained from Hg-rich samples investigated in this study are listed in Table 1, along with free volume percentages and actual masses of the constituent elements. Agreement between liquidus temperatures obtained at $x = 0.2$, $y = 0.5$ and 0.6 in this set of runs and those obtained in References 1 and 2 for the same x and y values is within experimental error. No correction has been made here for the free volume of Hg. The free volume and the masses of elemental constituents from which this correction can be calculated given a suitable thermodynamic model for the liquid are shown in Table 1.

The major sources of experimental uncertainty are subjectivity in selecting the proper liquidus point from a given DTA curve and random and systematic errors in the temperature measurements. The random temperature uncertainty as estimated from the scatter of the data points is typically $< \pm 1.0^{\circ}\text{C}$. The systematic error can be estimated by comparing the melting points of antimony and silver, measured in the DTA apparatus, with tabulated values. The melting point of Sb was always within 0.8°C of the tabulated value. The melting temperature of silver determined by placing a sample in place of the HgCdTe sample in the DTA apparatus was within 1°C of the tabulated value¹⁷ of 960.8°C . Thus the systematic uncertainty is estimated as $\pm 1.0^{\circ}\text{C}$. The uncertainty in reading the DTA is typically $\pm 0.5^{\circ}\text{C}$, yielding combined uncertainties of $\pm 2.5^{\circ}\text{C}$.

ORIGINAL PAGE IS
OF POOR QUALITY

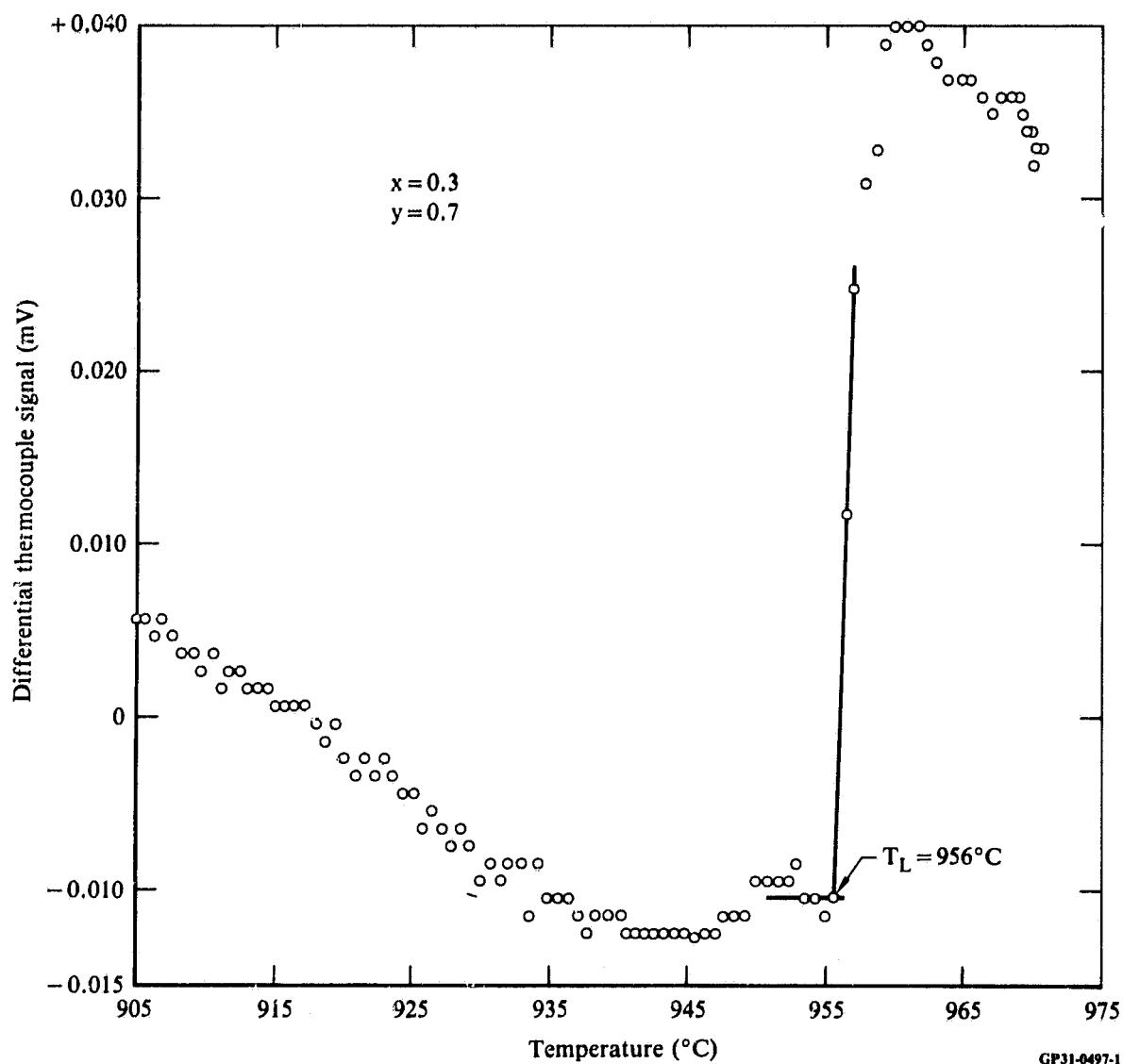


Figure 4. Thermogram of a typical HgCdTe differential-thermal-analysis experiment.

ORIGINAL PAGE IS
OF POOR QUALITY

TABLE 1. LIQUIDUS TEMPERATURES FOR Hg-RICH $(\text{Hg}_{1-x}\text{Cd}_x)_y\text{Te}_{1-y}$ ALLOYS.

x	y	Observed liquidus (°C)	Free volume inside ampule (%)	Mass of Hg (g)	Mass of Cd (g)	Mass of Te (g)
0.200	0.500	792.6 ± 2.0	—	—	—	—
0.2	0.5	792	—	(Reference 1)		
0.200	0.600	855.4 ± 2.9	—	11.553	1.619	6.107
0.2	0.6	849 ± 4	—	(Reference 16)		
0.099	0.751	858.5 ± 3.6	19	16.245	1.007	3.810
0.101	0.851	876.6 ± 2.0	*	18.409	1.143	2.286
0.201	0.701	914.7 ± 2.5	28	13.478	1.889	4.575
0.200	0.801	917.0 ± 2.0	*	15.404	2.157	3.045
0.299	0.703	956.3 ± 2.0	30	11.797	2.832	4.555
0.301	0.801	931.3 ± 1.5	*	13.480	3.237	3.050
0.300	0.900	902.4 ± 2.0	33	15.163	3.638	1.529
0.399	0.751	982.7 ± 2.6	29	10.830	4.044	3.810
0.401	0.851	949.9 ± 2.0	38	12.273	4.589	2.280

*Not available — sample exploded in DTA apparatus

GP31-0497-16

3. DIRECTIONAL SOLIDIFICATION OF $\text{Hg}_{1-x}\text{Cd}_x\text{Te}$ ALLOYS FROM PSEUDOBINARY MELTS

3.1 Alloy Preparation

$\text{Hg}_{1-x}\text{Cd}_x\text{Te}$ alloys were prepared by reacting stoichiometric amounts of the elements (99.9999% pure from Cominco American) in sealed, evacuated quartz ampules. Tubing dimensions were 5 mm i.d. x 10 mm o.d. Since crystals were to be grown by unidirectional solidification, the end of the ampule where solidification was to begin was tapered to facilitate the growth of a single crystal. A 4-mm diameter quartz rod was fused to this end of the ampule to serve as a support during crystal growth. After fabrication, the ampules were cleaned thoroughly, washed with a dilute solution of HF and HNO_3 , and annealed in vacuum at 1190°C .

The ampules were then loaded with appropriate amounts of the elements with excess Hg being added to compensate for the Hg vapor pressure over the melt. The ampules were evacuated, backfilled with He, and finally evacuated to a pressure less than 1 mPa (10^{-5} Torr) before being sealed.

After the ampules were sealed, the alloys were reacted in a horizontal rocking furnace. The loaded ampule was placed in the furnace, the rocking action was started, and the temperature was raised slowly ($1-2^\circ/\text{min}$) to 450°C and maintained at this temperature for several hours to accommodate the exothermic reaction of Hg, Cd, and Te. After this soak, the furnace temperature was raised to a temperature above the liquidus point of the alloy, where it was held for 18-24 hours.

At the completion of the reaction, the furnace motion was stopped with the tapered end of the ampule pointing downward, and power to the furnace was turned off. In this manner, three different alloys were prepared; L0750-27, L0750-35, and L0750-38, with $x = 0.2, 0.5,$ and 0.7 respectively.

3.2 Procedure for Directional Solidification

The precast alloys were regrown in the growth system shown in Figure 5. The ampule is mounted, with its tapered end down, atop a quartz pedestal and remains stationary during the growth process. Two resistively heated, tubular

ORIGINAL PAGE IS
OF POOR QUALITY

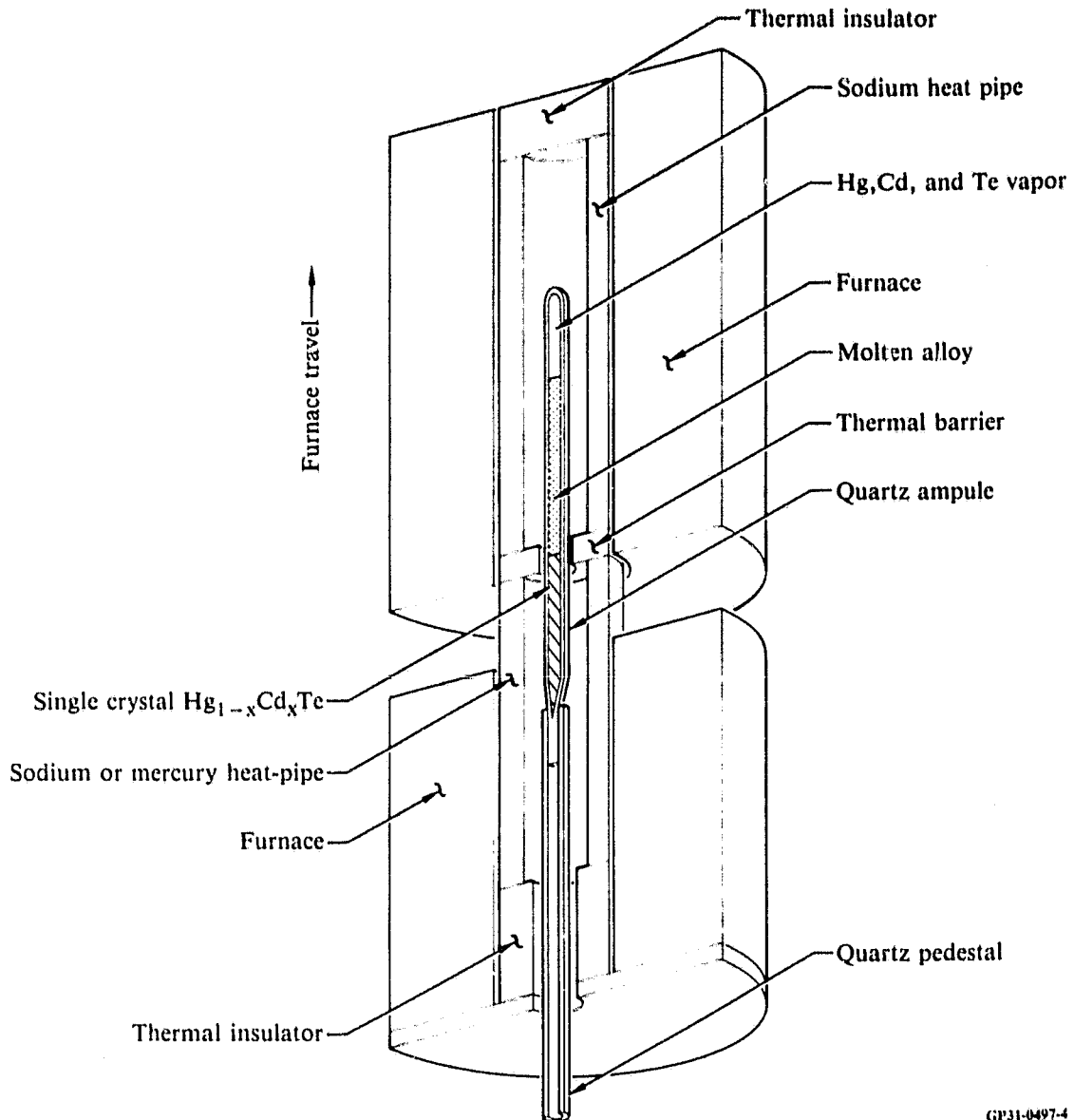


Figure 5. Bridgman-Stockbarger crystal-growth furnace assembly.

furnaces constitute a two-zone, traveling furnace system. Each temperature zone is lined with an isothermal heat-pipe furnace liner, and the zones are separated by a thermal insulating barrier. The temperature of the upper, hotter zone, T_u , is chosen so as to be above the liquidus temperature of the alloy. The temperature of the lower, cooler zone, T_l , is then set at the value determined by the relation

$$T_u^4 - T_{sol}^4 = T_{sol}^4 - T_l^4 ,$$

(1)

where T_{sol} is the solidus temperature. This choice of lower-zone temperature approximately balances the heat transfer in the upper and lower zones during the growth of the central region of the crystal.

Prior to each growth run, a thermocouple was inserted into the furnace system on a level with the bottom of the growth ampule. The furnace was then translated and the temperature was recorded as a function of furnace position.

At the beginning of the growth run, the furnaces were placed in their lowermost position, so that the sample was entirely within the hotter zone. This arrangement was maintained for several hours to ensure that the sample was completely molten and homogenized. The furnaces were then translated upward so that solidification began at the bottom of the ampule.

Crystal growth runs were completed for samples L0750-27, L0750-35, and L0750-38 with furnace translation rates of 0.59, 1.2, and 0.35 $\mu\text{m/s}$ respectively. The longitudinal temperature profiles for each run are shown in Figures 6, 7, and 8. Growth parameters are summarized in Table 2.

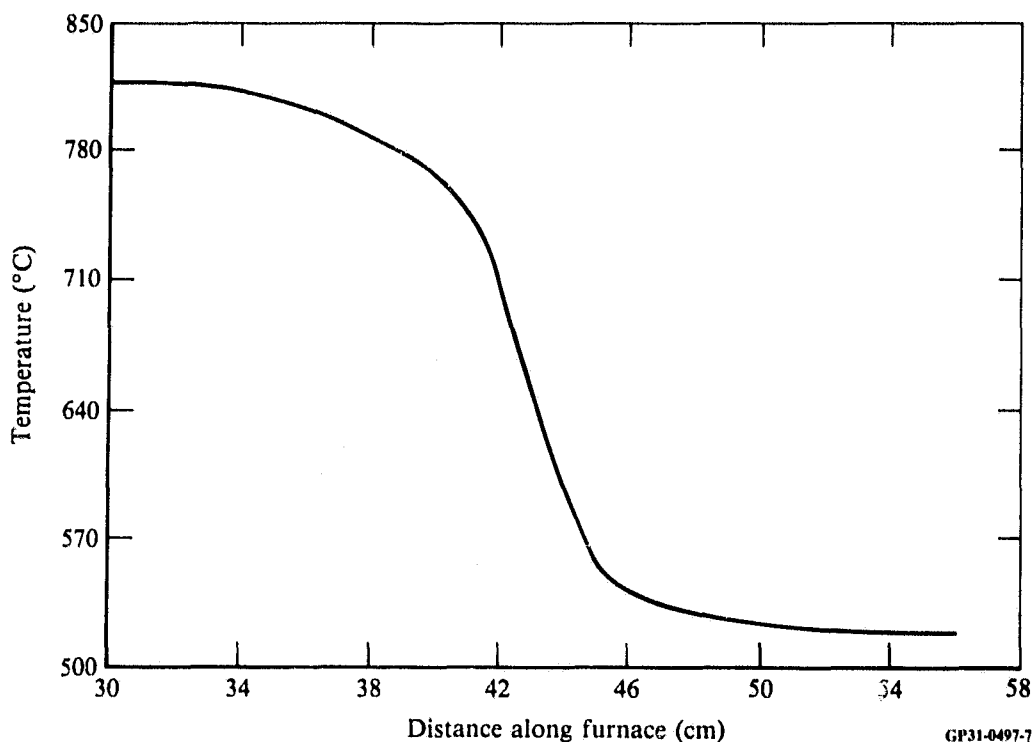


Figure 6. Furnace temperature profile for sample L0750-27.

ORIGINAL PAGE IS
OF POOR QUALITY

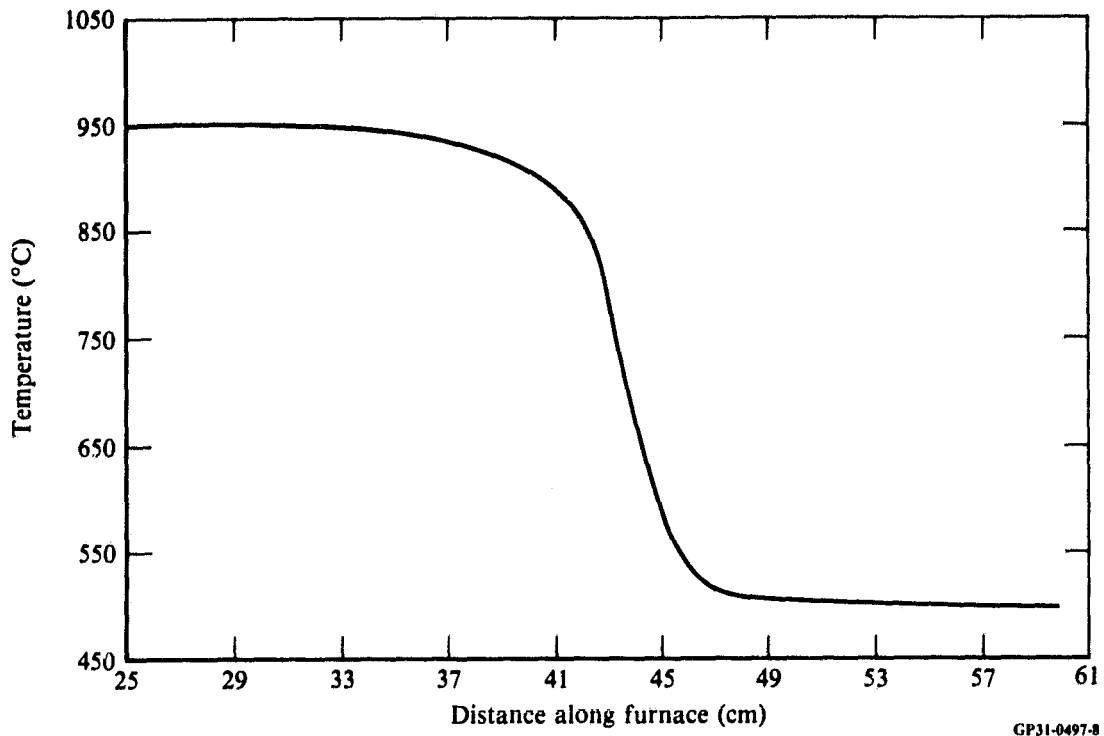


Figure 7. Furnace temperature profile for sample L0750-35.

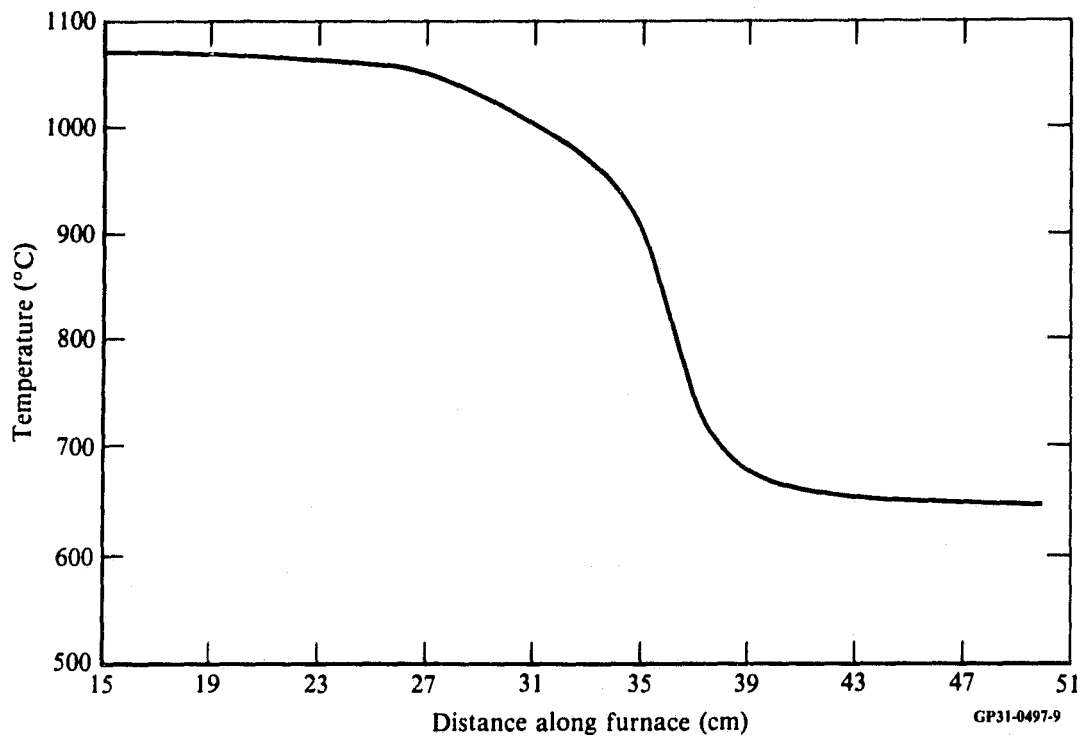


Figure 8. Furnace temperature profile for sample L0750-38.

TABLE 2. CRYSTAL-GROWTH PARAMETERS.

Sample	Composition, x	Lower zone Temp (°C)	Upper zone Temp (°C)	Barrier height (mm)	Growth rate (μm/s)
L0750-27	0.200	518	815	19	0.59
L0750-35	0.501	500	950	19	1.2
L0750-38	0.701	650	1070	19	0.35

GP31-0497-17

3.3 Determination of Alloy Composition by Mass Density Measurements

Since the cubic lattice constant, a_0 , of $\text{Hg}_{1-x}\text{Cd}_x\text{Te}$ varies so little with x , its measurement cannot be used for an accurate determination of alloy composition. Therefore, in this study, the average x -value of slices perpendicular to the growth axis were calculated from the measured mass densities and the cubic lattice constant data of Wolley and Ray.¹⁸

The lattice constant data of Wolley and Ray can be represented as a function of x by

$$a_0 = 0.646153 + (0.73671 x + 1.90501 x^2 - 0.69347 x^3)/1000 \quad (2)$$

where a_0 is the cubic lattice constant in nanometers. In the zincblende crystal structure there are 4 atoms of each type per unit cell. Since this is a pseudobinary alloy, the Hg and Cd together comprise one type of atom. Thus in each unit cell there are $4x$ Cd atoms, $4(1-x)$ Hg atoms, and 4 Te atoms. Since this is a cubic structure, the volume of the unit cell is simply given by a_0^3 , and thus the density, ρ_m , is related to the lattice constant and composition by

$$\rho_m = \frac{4xM_{\text{Cd}} + 4(1-x)M_{\text{Hg}} + 4M_{\text{Te}}}{a_0^3} \quad (3)$$

where M_{Cd} , M_{Hg} , and M_{Te} are the atomic masses of Cd, Hg, and Te, respectively. For a given density, the value of x can be determined by simultaneously solving Equations (2) and (3).

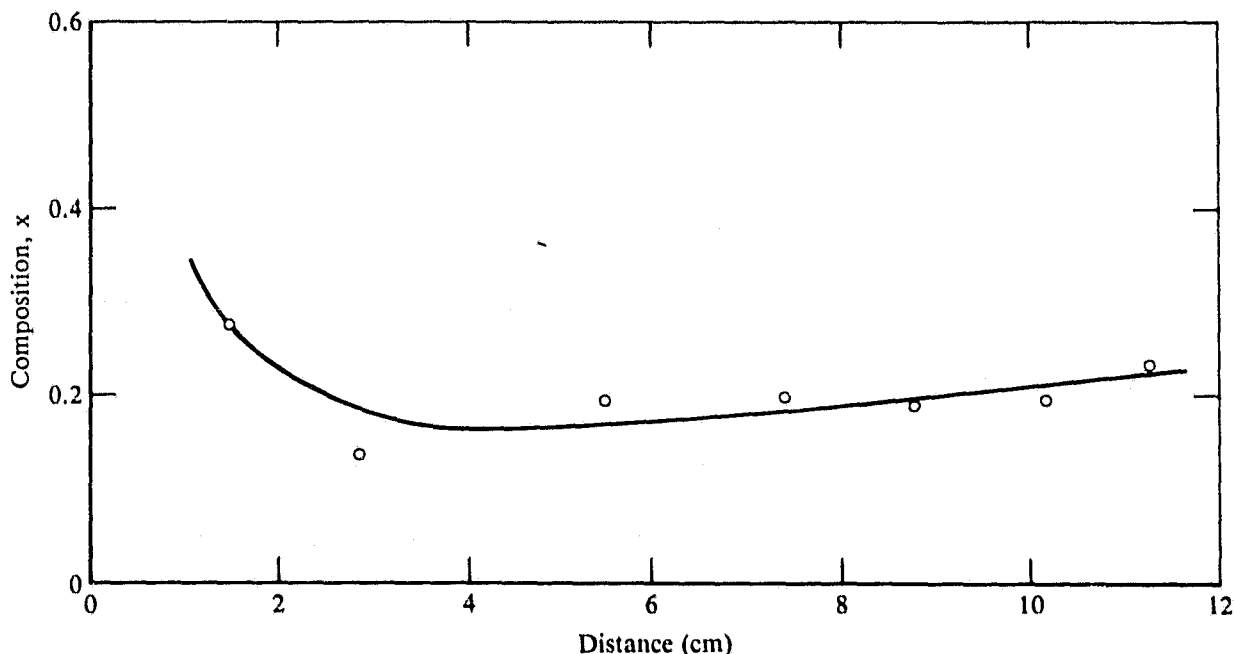
ORIGINAL PAGE IS
OF POOR QUALITY

The mass density of a sample was determined by obtaining its weight in air, W_a , and its weight when immersed in water, W_w . The density is then given by

$$\rho_m = \frac{W_a \rho_w - W_w \rho_a}{W_a - W_w} \quad (4)$$

where ρ_w is the mass density of water and ρ_a is the mass density of air. The procedure used was that described by Bowman and Schooner,¹⁹ in which the sample is immersed in water and briefly boiled to eliminate gases dissolved in the water and minute air bubbles that may be trapped on the sample. The sample is then weighed while immersed, and weighed again in air. The density of water and air are calculated as described in Reference 19 using the parameters: water temperature, air temperature, barometric pressure, depth of immersion of the sample, and elapsed time since boiling.

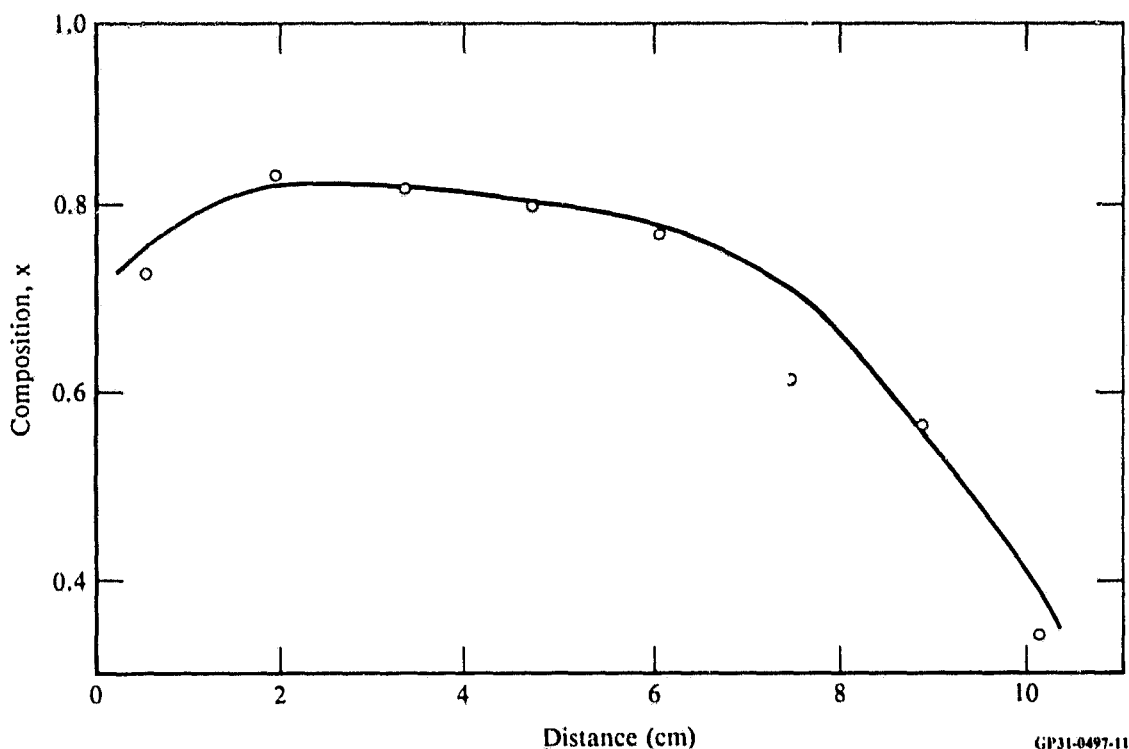
The alloy compositions of crystals L0750-27 ($x = 0.2$) and L0750-38 ($x = 0.7$) as functions of position on the growth axis are shown in Figures 9 and 10. Crystal L0750-35 ($x = 0.5$) was porous and brittle, and it was not examined further.



GP31-0497-10

Figure 9. Composition profile of sample L0750-27.

ORIGINAL PAGE IS
OF POOR QUALITY



GP31-0497-11

Figure 10. Composition profile of sample L0750-38.

3.4 Determination of Alloy Composition by Infrared Transmission Measurements

To determine the radial homogeneity of a given slice, attempts were made to determine the infrared transmission spectrum of the slice as a function of position on the slice. This was accomplished by using an infrared spectrophotometer (Perkin-Elmer model 457) equipped with a 1-mm diameter measuring aperture and a translating sample holder. The approximate bandgap energy, E_g , was determined by choosing the energy at which the sample exhibited 50% transmittance. This energy was then used in the equation of Scott²⁰:

$$E_g = 0.303 + 1.73x + 5.6 \times 10^{-4}(1 - 2x)T + 0.25 x^4, \quad (4)$$

which was then solved for x . The spectrometer is capable of mapping only samples with x values < 0.4 , because of its limited wavelength range, and thus only slices from L0750-27 were examined.

ORIGINAL PAGE IS
OF POOR QUALITY

The slices from L0750-27, as grown, were found to be opaque because of their highly p-type character. To reduce the hole carrier concentration, the slices were annealed in Hg vapor. Several slices were simultaneously annealed in a pyrex tube with a constriction to separate the samples from the Hg liquid used to provide the Hg annealing atmosphere. The tube was evacuated to 0.1 mPa (10^{-6} Torr) before being sealed. In this manner, slices from ingot L0750-27 were annealed in Hg vapor at 325°C for 114 h. The annealing treatment failed to yield infrared-transparent samples.

3.5 Electrical Characterization

Since none of the ingots described previously could be assessed for radial homogeneity, samples for electrical characterization were taken from a 5-mm diameter residual ingot, L0721-37, previously grown for the McDonnell Douglas Corporation Independent Research and Development program.

Ingot L0721-37 was grown by the Bridgman-Stockbarger method as was described previously. Crystal growth parameters for ingot L0721-37 are given in Table 3. After a Hg anneal of 63.5 h at 325°C, the slices chosen were mapped as described previously. The results are shown in Figures 11 and 12. Due to the severe radial inhomogeneity of these samples near the edges of the slices, a 3 x 3 mm sample was taken from L0721-37-2, and electrical measurements were performed on this sample

The electrical resistivity and Hall coefficient measurements were made by the method of van der Pauw.²¹ Following attachment of the electrical leads with indium, the samples were fastened to the sample block of a closed-cycle helium refrigerator, which is an integral part of an MDRL-designed automated

TABLE 3. CRYSTAL-GROWTH PARAMETERS FOR INGOT L0721-37.

Composition, x	Lower zone Temp (°C)	Upper zone Temp (°C)	Barrier height (mm)	Growth rate ($\mu\text{m/s}$)
0.303	206	894	38	0.23

GP31-0497-18

ORIGINAL PAGE IS
OF POOR QUALITY

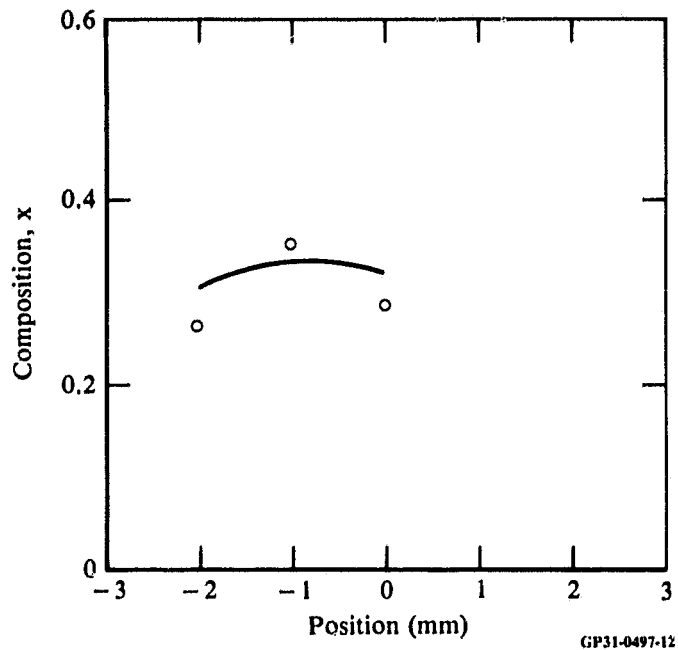


Figure 11. Radial composition of sample L0721-37-1.

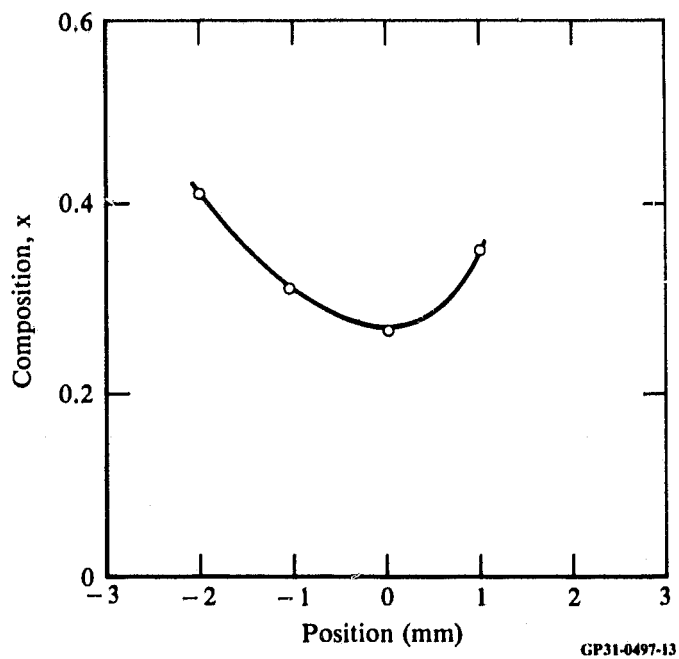


Figure 12. Radial composition of sample L0721-37-2.

ORIGINAL PAGE IS
OF POOR QUALITY

galvanomagnetic data acquisition system. A block diagram of the system is shown in Figure 13. The entire experiment, including temperature variation and magnetic field direction, is controlled by a microcomputer (Digital Equipment Corp. MINC-11).

The measured Hall electron concentrations and Hall electron mobilities for sample L0721-37-2 are shown in Figures 14 and 15, respectively. As can be seen, the sample has been annealed to n-type. The electron mobilities are extremely low, and evidently the sample is heavily compensated. Furthermore, the temperature dependences of the Hall concentration and mobility indicate that either the compositional uniformity is low or the sample did not reach equilibrium during the annealing.

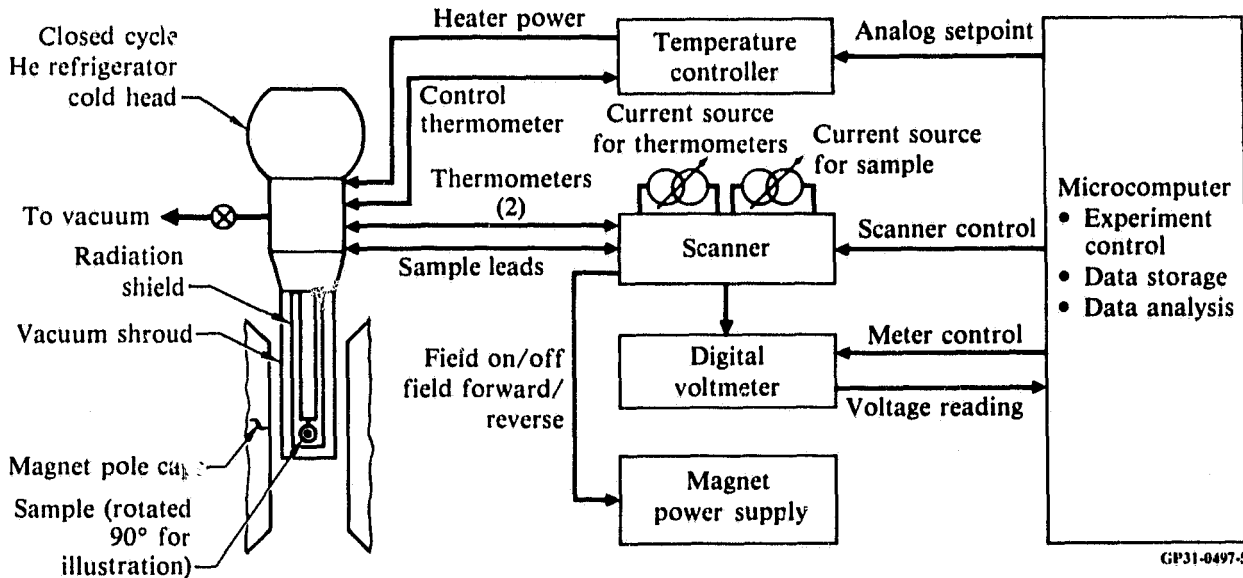


Figure 13. Block diagram of automated system for measurements of galvanomagnetic properties of semiconductors.

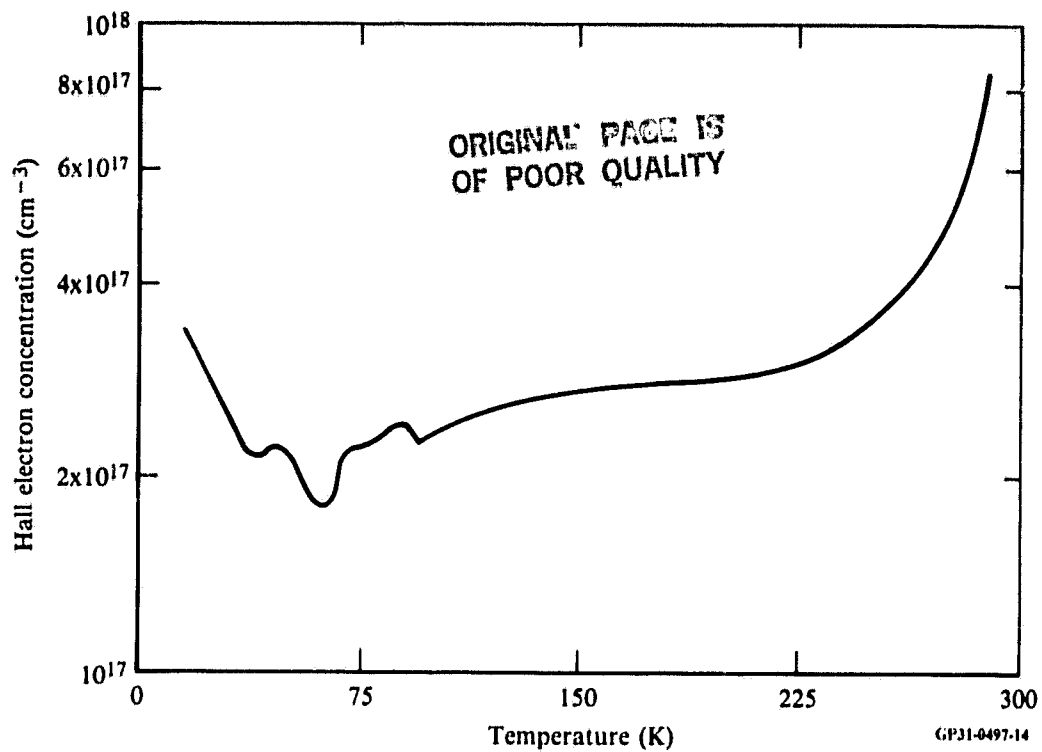


Figure 14. Hall electron concentration for sample L0721-37-2.

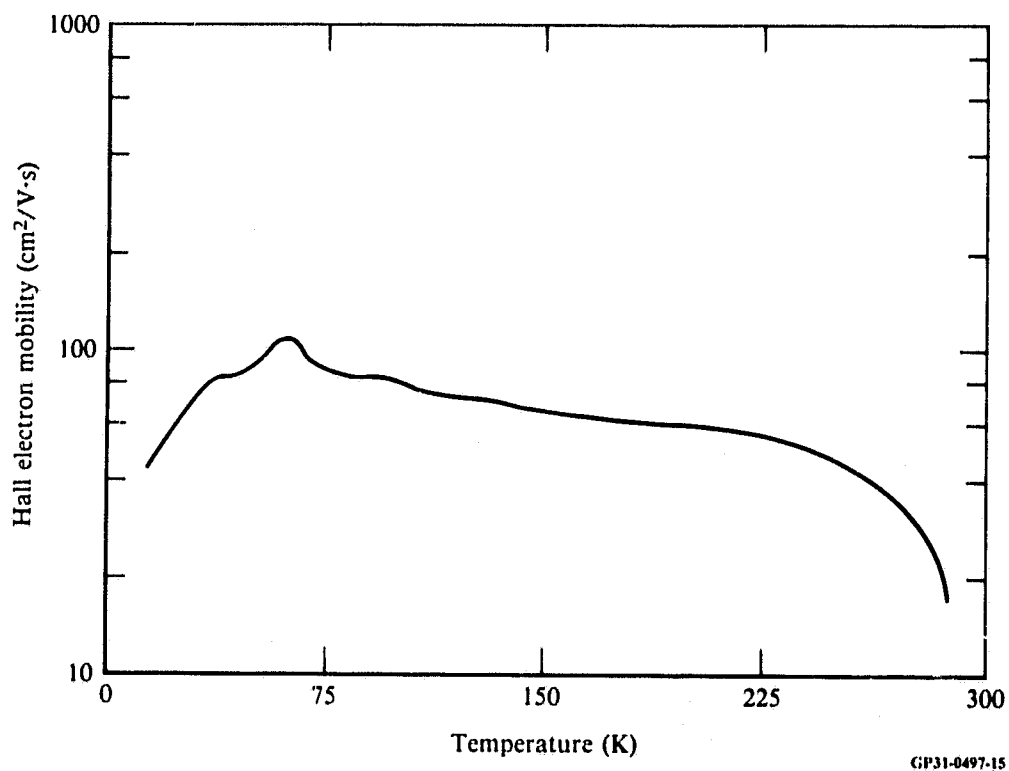


Figure 15. Hall electron mobility for sample L0721-37-2.

REFERENCES

1. S. L. Lehoczky, F. R. Szofran, and B. G. Martin. Advanced Methods for Preparation and Characterization of Infrared Detector Materials. Interim Report, NASA Contract No. NAS8-33107 (July 1980).
2. F. R. Szofran and S. L. Lehoczky. The HgTe-CdTe Pseudobinary Phase Diagram. J. of Electron. Mat. 10, 1131 (1980).
3. S. L. Lehoczky, C. J. Summers, and F. R. Szofran. Directional Solidification and Characterization of $\text{Hg}_{1-x}\text{Cd}_x\text{Te}$ ($x < 0.25$). NATO Cadmium Mercury Telluride (CMT) Workshop, Grenoble, France, 23-24 April 1980.
4. A. S. Jordan. A Theory of Regular Associated Solutions Applied to the Liquidus Curves of the Zn-Te and Cd-Te Systems. Met. Trans. 1, 239 (1970).
5. S. Szapiro. Solid-Liquid Equilibria in Ternary Regular Associated Solutions. J. Electron. Mat. 5, 223 (1976).
6. A. J. Strauss. M.I.T. Lincoln Lab., private communication.
7. B. M. Kulwicki. The Phase Equilibria of Some Compound Semiconductors by DTA Calorimetry. Ph.D. Dissertation, Univ. of Michigan (1963).
8. M. R. Lorenz. Phase Equilibria in the System Cd-Te. J. Phys. Chem. Solids 23, 939 (1962).
9. J. Steininger, A. J. Strauss, and R. F. Brebrick. Phase Diagram of the Zn-Cd-Te Ternary Systems. J. Electrochem. Soc. 117, 1305 (1970).
10. J. Steininger. Hg-Cd-Te Phase Diagram Determination by High Pressure Reflux. J. Electron. Mat. 5, 299 (1976).
11. V. G. Smith, W. A. Tiller, and J. W. Rutter. A Mathematical Analysis of Solute Redistribution During Solidification. Can. J. Phys. 33, 723 (1953).
12. S. L. Lehoczky and F. R. Szofran. Diffusion-Limited Directional Solidification of $\text{Hg}_{0.8}\text{Cd}_{0.2}\text{Te}$. Fifth International Conference on Vapor Growth and Fifth American Conference on Crystal Growth, Coronado, California, 19-24 July 1981.
13. S. L. Lehoczky, J. G. Broerman, D. A. Nelson, and C. R. Whitsett. Temperature-Dependent Electrical Properties of HgSe. Phys. Rev. B 9, 1598 (1974).

14. D. A. Nelson, J. G. Broerman, C. J. Summers, and C. R. Whitsett. Electrical Transport in the $\text{Hg}_{1-x}\text{Cd}_x\text{Te}$ Alloy System. Phys. Rev. B 18, 1658 (1978).
15. E. O. Kane. Band Structure of Indium Antimonide. J. Phys. Chem. Solids 1, 249 (1957).
16. S. L. Lehoczky and F. R. Szofran. Advanced Methods for Preparation and Characterization of Infrared Detector Materials. Interim Report, NASA Contract No. NAS8-33107 (September 1981).
17. R. Hultgren, P. D. Desai, D. T. Hawkins, M. Gleiser, K. K. Kelley, and D. D. Wagman. Selected Values of the Thermodynamic Properties of the Elements, (American Society for Metals, Metals Park, OH, 1973).
18. J. C. Wolley and B. Ray. Solid Solutions in $\text{A}^{\text{II}}\text{B}^{\text{VI}}$ Tellurides. J. Phys. Chem. Solids, 13, 151 (1960).
19. H. A. Bowman, R. M. Schooner, and M. W. Jones. Procedure for High Precision Density Determinations by Hydrostatic Weighing. J. Res. Natl. Bur. Std. (U. S.), 71C, 179 (1967).
20. M. W. Scott. Energy Gap in $\text{Hg}_{1-x}\text{Cd}_x\text{Te}$ by Optical Absorption. J. Appl. Phys., 40, 4077 (1969).
21. L. J. van der Pauw. A Method of Measuring Specific Resistivity and Hall Effects of Discs of Arbitrary Shape. Philips Research Reports, 13, 1 (1958).

ORIGINAL PAGE IS
OF POOR QUALITY